IEEE Access
Multidisciplinary | Rapid Review | Open Access Journal

Received July 19, 2017, accepted August 8, 2017, date of publication August 15, 2017, date of current version February 28, 2018.

Digital Object Identifier 10.1109/ACCESS.2017.2740323

Generation of Wideband Tunable Orbital Angular Momentum Vortex Waves Using Graphene Metamaterial Reflectarray

YAN SHI, (Senior Member, IEEE), AND YING ZHANG
School of Electronic Engineering, Xidian University, Xi'an 710071, China

Corresponding author: Yan Shi (e-mail: shiyan@mail.xidian.edu.cn)

This work was supported in part by the National Natural Science Foundation of China under Contract 61771359, in part by the Technology Innovation Research Project of the CETC, and in part by the Fundamental Research Funds for the Central Universities under Grant SPSZ031410.

ABSTRACT In this paper, a wideband tunable reflectarray consisting of a graphene-based metamaterial structure has been developed to generate an orbital angular momentum (OAM) vortex wave in terahertz. In the proposed reflectarray, a multi-layer graphene metamaterial unit cell is designed, and through varying chemical potentials of the graphene sheets, reflection phase range of 360° and reflection magnitude better than −2.5 dB can be achieved. By suitably choosing the chemical potentials of the graphene layers, the designed reflectarray can produce the OAM vortex waves with $l = \pm 1, \pm 2$, and ± 3 modes. Moreover, the OAM beams operating in a wide frequency band from 1.8 to 2.8 THz can be generated with the adjustment of the chemical potentials. Simulation results demonstrate good performance of the proposed reflectarray in the efficient generation and manipulation of the OAM vortex waves, which is promising to be used in wireless communication.

INDEX TERMS Graphene, orbital angular momentum (OAM), wideband, tunable.

I. INTRODUCTION

Nowadays, rapid development of wireless communication is facing serious challenges due to scarce spectrum resources and limited polarization modes. How to efficiently improve channel capacity of communication systems has been concerned. Orbital angular momentum (OAM) vortex waves have attracted much attentions since Allen *et al*. found that light beam with an azimuthal phase dependence of $\exp(il\varphi)$ carries an OAM, in which φ represents the azimuthal angle and l is the topological charge [1]. With a theoretically unlimited range of orthogonal eigenstates, the OAM is regarded as a promising way to increase communication capacity and spectral efficiency.

Various methods have been proposed to generate the vortex waves carrying the OAM, for instance antenna array [2], spiral phase plate (SPP) [3], [4], holographic plate [5], and angular gratings [6], etc. Among them, metamaterials have been used to generate the OAM beams from microwave to optical frequencies due to their unusual properties not found in natural media. A plasmonic metasurface composed of V-sharp antennas, which was first proposed in [7], has been used to generate optical OAM [8]. More recently, a single OAM beam was generated by some metamaterial structures including a tri-dipole unit cell [9], a circular patch with metallic via holes [10], a dielectric drilled by air holes [11], and multiple spiral phase surfaces [12], etc. In addition, a square-patch metasurface was proposed to generate multiple OAM beams at 5.8GHz [13]. However, to the best of our knowledge, the OAM vortex waves have been generated, in all the reported references, with fixed mode operation.

In recent years, interest in graphene has rapidly grown due to its remarkable properties. Graphene is an allotrope of carbon in the form of a two-dimensional, atomic-scale, hexagonal lattice. By controlling voltage applied to the graphene via external gate, the chemical potential of the graphene can be flexibly adjusted, and thus its surface impedance can be controlled. With these unique properties, graphene-based reflectarray antenna [14], tunable absorber [15], and nonlinear optical device [16] have been developed. In this paper, we use the graphene to design a reflectarray for generating wideband OAM vortex waves with tunable modes. A multilayer metamaterial unit cell consisting of SiO_2, Al_2O_3, graphene and Au materials is proposed to achieve a reflection phase of 360°. With the adjustment of the chemical potential

of the graphene, the proposed reflectarray can generate OAM beams with $l = \pm 1, \pm 2$ and ± 3 modes, and furthermore the resultant OAM beams can operate in a wide band from 1.8THz to 2.8THz. Simulation results are given to validate the proposed design.

II. DESIGN OF GRAPHENE-BASED METAMATERIAL REFLECTARRAY

In terahertz, a monolayer graphene is regarded as an infinitesimally thin conductive layer, whose surface conductive can be written according to the semiclassical Kubo formula [17]–[19]:

$$\sigma(\omega, \mu_c, \Gamma, T) = \sigma_{intra}(\omega, \mu_c, \Gamma, T) + \sigma_{inter}(\omega, \mu_c, \Gamma, T) \tag{1}$$

where intra-band conductivity σ_{intra} and inter-band conductivity σ_{inter} are defined as, respectively

$$\begin{cases} \sigma_{intra}(\omega, \mu_c, \Gamma, T) \approx i\dfrac{e^2 k_B T}{\pi\hbar^2(\omega + i2\Gamma)} \times \left[\dfrac{\mu_c}{k_B T} + 2\ln\left(e^{-\frac{\mu_c}{k_B T}} + 1\right)\right], \\ \sigma_{inter}(\omega, \mu_c, \Gamma, T) \approx i\dfrac{e^2}{4\pi\hbar}\ln\left[\dfrac{2|\mu_c| - (\omega + i2\Gamma)\hbar}{2|\mu_c| + (\omega + i2\Gamma)\hbar}\right]. \end{cases} \tag{2}$$

Here e is electron charge, k_B is Boltzmann constant, $\hbar$ is reduced Planck's constant, ω is radian frequency, $\Gamma = 0.32\ meV$ represents charged particle scattering rate, $T = 300\ K$ is room temperature, and μ_c is defined as chemical potential of graphene.

According to Pauli exclusion principle, the inter-band contribution of the graphene conductivity can be neglected safely in the case of lower THz frequency and room temperature. Hence, the surface impedance of the graphene can be calculated approximately as $Z \approx 1/\sigma_{intra}$. In order to tune the surface impedance of the graphene sheet, an external gate voltage V_A is applied to the graphene. With the external voltage, the chemical potential μ_c of the graphene can be estimated by the following formula [20]:

$$|\mu_c| \approx \hbar v_F \left\{\pi a_0 |V_A - V_{Dirac}|\right\}^{1/2}, \tag{3}$$

in which the Fermi velocity of the Dirac fermions is $v_F \approx 9\times10^5\ m/s$, the constant estimated through a single capacitor model is $a_0 \approx 9\times10^{16}\ m^{-2}V^{-1}$, and the Dirac voltage offset caused by the natural doping is $V_{Dirac} = 0.8\ V$.

In order to convert a plane wave into an OAM beam with the lth mode using a reflectarray, an ideal helical phase profile $\exp(il\varphi)$ on the reflection surface is desired. Here we uniformly divide the whole reflectarray into N regions along the azimuthal angle. In ith region, the corresponding sub-reflectarray provides the reflection phase of $2\pi li/N$ $(i = 1, \cdots, N)$ so that the whole reflectarray can approximately achieve the helical phase profile of $\exp(il\varphi)$. It is worthwhile noting that the number of the regions is chosen to guarantee the approximately continuous variation of the reflection phase. In the proposed reflectarray shown in Fig. 1(a), we use $N = 12$. To obtain desirable reflection phase in each region, a novel metamaterial unit cell is designed. As shown in Fig. 1(b), the proposed unit cell is a multilayer sandwich structure with a period of $P = 20\ \mu$m. Each sandwich structure consists of graphene/Al_2O_3/SiO_2 materials from the top to the bottom. An insulating layer of Al_2O_3 material is placed between two adjacent sandwich structures. The thicknesses of SiO_2 and Al_2O_3 materials are 12 μm and 10 nm, respectively. The bottom of the unit cell is an Au material as a reflective ground. Thickness of the Au material is chosen as 5 μm, which is larger than the largest skin depth in THz. In order to adjust the chemical potentials of the graphene materials in the proposed unit cell, an external DC voltage is applied between the graphene layer and the SiO_2 layer in each sandwich structure. Hence three chemical potentials and the three corresponding surface impedances of the graphene layers in the unit cell can be controlled. For convenience, we denote the chemical potentials of the graphene layers from the top to the bottom as 'μ_{c1}', 'μ_{c2}' and 'μ_{c3}', respectively.

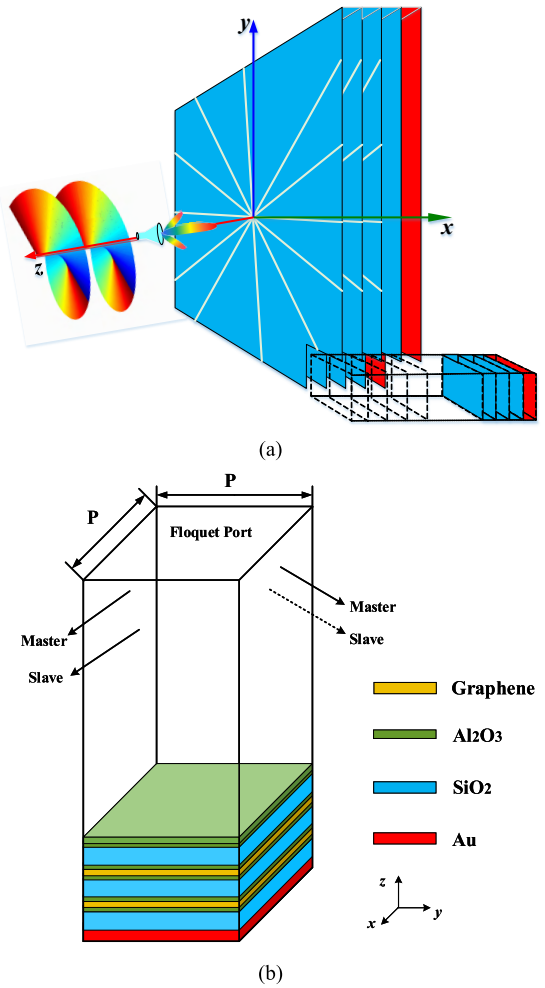

FIGURE 1. Reflectarray for generation of the OAM beam. (a) Structure of reflectarray. (b) Graphene-based unit cell.

To demonstrate the performance of the proposed unit cell, we use a full-wave finite-element solver to simulate its

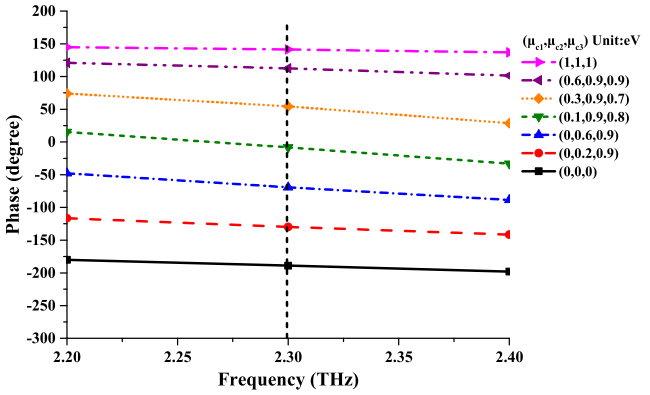

FIGURE 2. Variation of reflection phases with the frequency and the chemical potentials of the graphene.

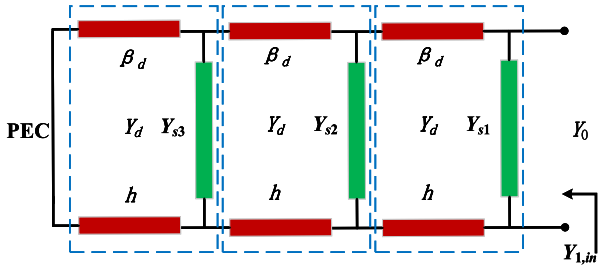

FIGURE 3. Equivalent network of the proposed unit cell.

reflection phase [22]. As shown in Fig. 1(b), the periodic boundary conditions (PBCs) are employed to simulate the infinite periodic cells. In the simulation, 1st-order vector basis functions are used. Fig. 2 demonstrates the variation of the reflection phases of the proposed unit cell with the frequency and the chemical potentials of three graphene layers. It can be seen from Fig. 2 that at 2.3THz, the reflection phase range of the unit cell approximately reaches 360° as the chemical potentials vary. Moreover, when the change of the operating frequency is in a small range, i.e., from 2.2 THz to 2.4 THz, the reflection phases approximately keep unchanged with the fixed chemical potentials of three graphene layers.

In order to further explore the performance of the proposed unit cell, a transmission line equivalent network is developed, as shown in Fig. 3. In the designed unit cell, each sandwich structure composed of graphene/Al_2O_3/SiO_2 materials from the top to the bottom can be equivalent to a transmission line segment with a shunt admittance of Y_{si} $(i = 1, 2, 3)$. Considering that the thickness of the Al_2O_3 material is much smaller than that of the SiO_2 material, the effect of the Al_2O_3 material can be neglected. Hence the propagation constant of the transmission line segment β_d is the phase constant in the SiO_2 material and the length of the transmission line segment h becomes the thickness of the SiO_2 material. The graphene material is characterized as the shunt admittance. The whole equivalent network can be obtained by cascading the equivalent network of each sandwich structure.

Following the microwave network analysis [23], we have

$$S_{11} = \frac{Y_0 - Y_{1,in}}{Y_0 + Y_{1,in}}, \tag{4}$$

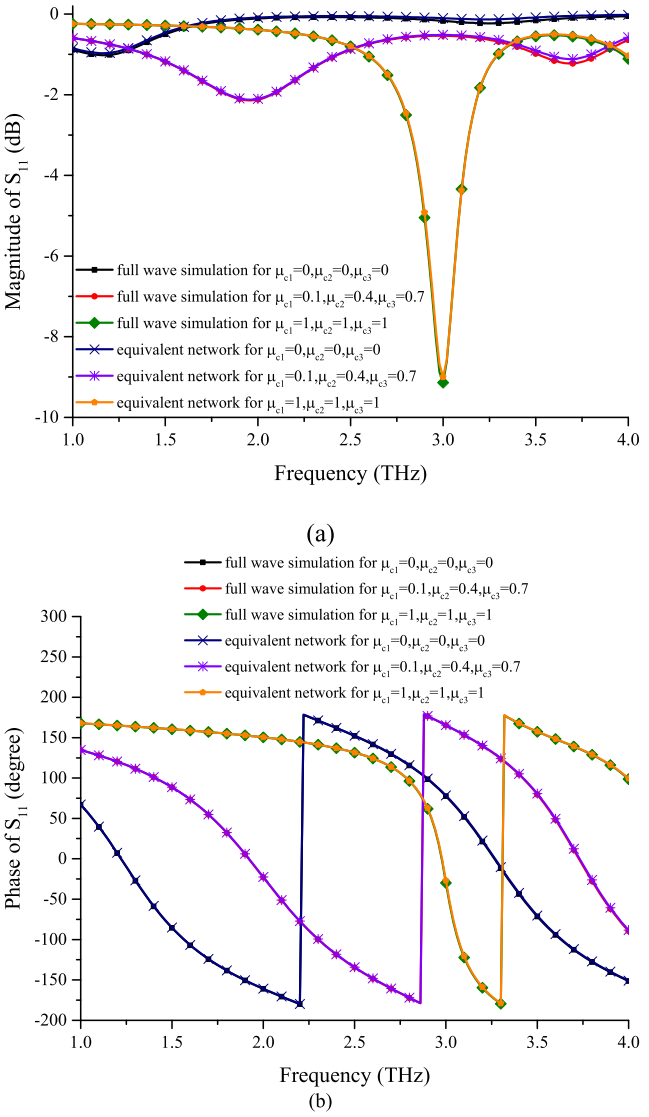

FIGURE 4. Performance comparison between the equivalent network and the full-wave simulation. (a) Magnitude of S_{11}. (b) Phase of S_{11}.

where

$$Y_{i,in} = Y_{s_i} + Y_d \cdot \frac{Y_{i+1,in} + jY_d \tan(\beta_d h)}{Y_d + jY_{i+1,in} \tan(\beta_d h)} \quad (i = 1, 2), \tag{5}$$

$$Y_{3,in} = Y_{s3} - jY_d \cot(\beta_d h). \tag{6}$$

Fig. 4 shows the comparison of the S parameter obtained by the equivalent network and the full-wave simulation. Good agreement between two results validates the proposed equivalent network. With the use of the proposed equivalent network, we study the wideband performance of the proposed unit cell. The reflection phases of the proposed unit cell are solved from 1.8THz to 2.8 THz, as the chemical potential of each graphene layer varies from 0 eV to 1 eV. As shown in Fig. 5, when the chemical potentials of three graphene layers are suitably chosen, the resultant reflection phase range can well cover 360° in the wide frequency band.

With the designed unit cell, the reflectarray is constructed, as shown in Fig. 6(a). In each region of the reflectarray,

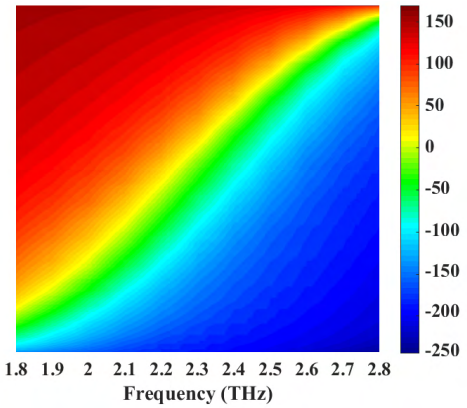

FIGURE 5. Reflection phase range for all possible chemical potentials of three graphene layers in a wide frequency band from 1.8THz to 2.8THz.

TABLE 1. Design parameters in each different region.

Region	1	2	3	4	5	6
μ_{c1}(eV)	0	0.1	0.1	0.1	0	0
μ_{c2}(eV)	0	0	0.2	0.4	0.6	0.8
μ_{c3}(eV)	0	0.6	0.9	0.7	0.9	1
Phase(°)	-189	-159	-129	-99	-69	-37
S_{11}(dB)	-0.07	-0.46	-0.30	-1.13	-1.37	-1.46
Region	**7**	**8**	**9**	**10**	**11**	**12**
μ_{c1}(eV)	0.1	0.2	0.3	0.4	0.6	1
μ_{c2}(eV)	0.9	0.9	0.9	0.9	0.9	1
μ_{c3}(eV)	0.8	0.7	0.7	1	0.9	1
Phase(°)	-8	23	54	84	112	141
S_{11}(dB)	-1.87	-2.24	-2.14	-1.58	-1.13	-0.55

the same metamaterial unit cell is used. Meanwhile, in order to ensure the insulation between two adjacent regions, a small height difference Δh is introduced, as shown in Fig. 6(b). The whole size of the designed reflectarray is set as $10\lambda \times 10\lambda$, where λ is the wavelength in free space at the center frequency of 2.3 THz. Note that the reflectarray size of 10λ is large enough to neglect the effect of the edge diffraction. In order to generate an OAM beam with the $l = 1$ mode at 2.3THz, the chemical potentials of the graphene layers in each region are shown in Table 1. The reflection magnitude and phase of the resultant metamaterial unit cell are given in Table 1. It can be seen that the difference of the reflection phases between two adjacent regions is 30°, and thus the reflection phase approximately achieves a continuous 2π change from $-189°$ to 141° in a counterclockwise direction. The reflection magnitudes of all regions are better than -2.5dB. Here a wideband horn antenna as the excitation is used to generate a wave incident on the reflectarray. The horn antenna is located at center of the reflectarray. The distance between the horn antenna and the reflectarray is chosen as 8λ. Numerical results shown in Fig. 7(a) demonstrate the simulated OAM vortex waves with the $l = 1$ mode generated by the proposed reflectarray. The spiral phase distributions are observed. Furthermore, when the chemical potentials

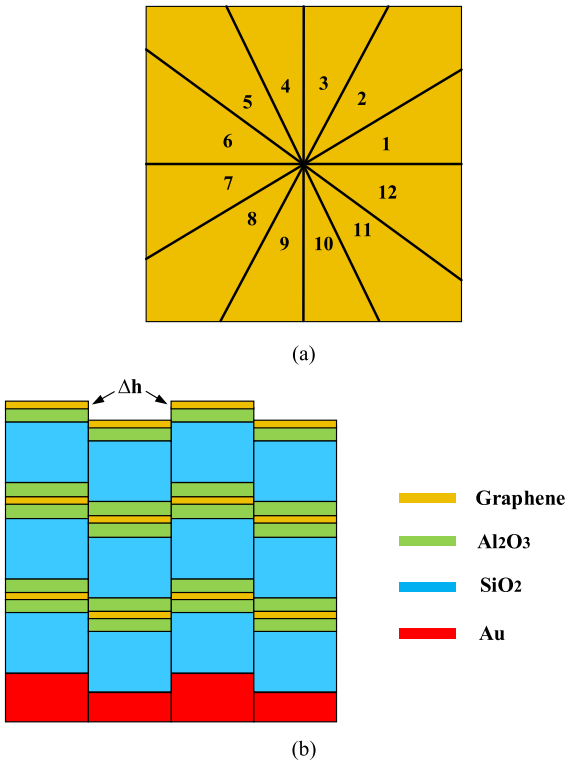

FIGURE 6. Schematic diagram of the designed reflectarray. (a) The whole array divided into twelve regions, each of which is filled by the same metamaterial unit cells. (b) The side view of the reflectarray.

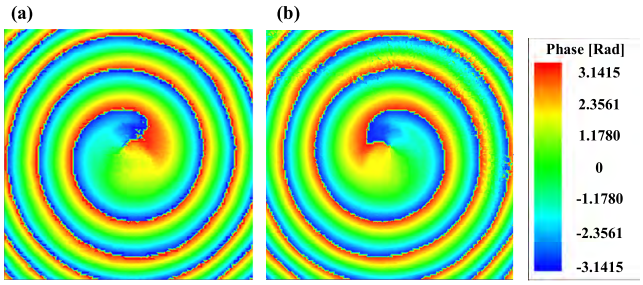

FIGURE 7. Simulated OAM beams with the $l = \pm 1$ mode by using the reflectarray. (a) $l = 1$. (b) $l = -1$.

of the graphene layers in twelve regions are re-arrayed in a clockwise direction, the OAM vortex wave with the $l = -1$ mode is generated, as shown in Fig. 7(b).

In order to generate the OAM beams with the higher modes, the difference of the reflection phases between two adjacent regions increases multiplicatively. For an OAM beam with the lth mode, the desired reflection phase interval between two adjacent regions is $2\pi l/N$. Considering $N = 12$ in this paper, the phase interval becomes $l\pi/6$. Therefore, the reflection phase intervals for the OAM beams with the $l = \pm 1$, $l = \pm 2$, and $l = \pm 3$ modes are $\pm 30°$, $\pm 60°$, and $\pm 90°$, respectively. In this scenario, the chemical potentials of the graphene sheets for the generation of the OAM beams with the higher modes can be easily obtained according to those used to generate the OAM beam of the $l = 1$ mode. For example, for the OAM beam with $l = 2$ mode, the chemical potentials of the graphene layers in

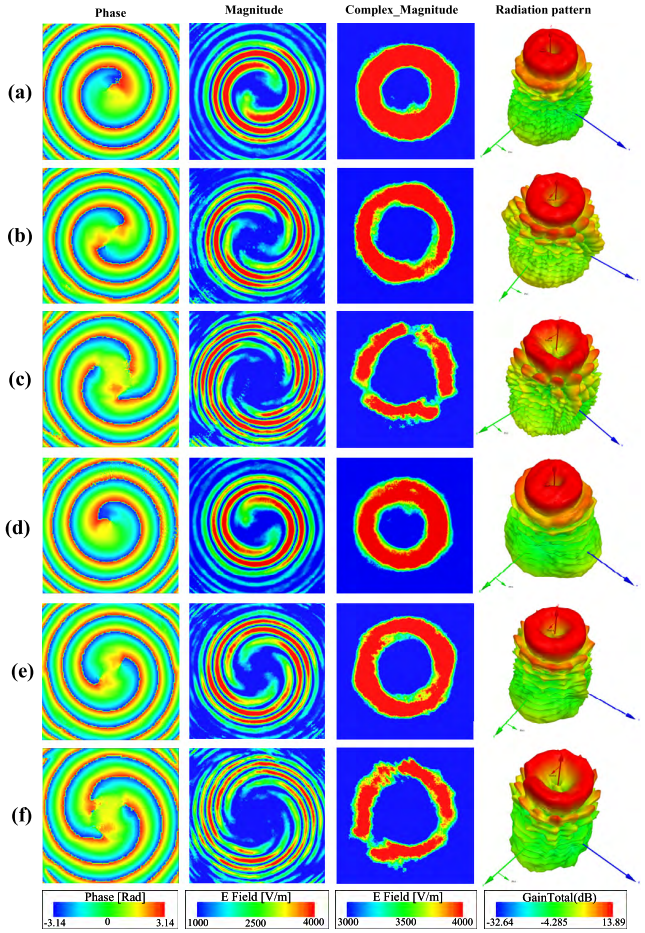

FIGURE 8. The OAM beams with the different modes. (a) $l = 1$. (b) $l = 2$. (c) $l = 3$. (d) $l = -1$. (e) $l = -2$. (f) $l = -3$.

ith region ($i = 1, 2, \cdots, 6$) are same as those in $(2i - 1)$th region of Table 1. The chemical potentials of the graphene layers in remaining regions are same as those in the former regions in a rotationally symmetry way. Fig. 8 demonstrates the OAM vortex waves with different modes at 2.3 THz. It can be seen from Fig. 8 that the spiral phase distributions of the OAM vortex waves with $l = \pm 1$, $l = \pm 2$, and $l = \pm 3$ modes can be clearly observed, and the doughnut-shaped intensity distributions are obtained. The radiation patterns with the singularity in the center are illustrated in Fig. 8. With this characteristic, the coupling between the reflective wave and the feed antenna is greatly weakened.

In order to evaluate the purity of different OAM modes, spectral analysis of Fourier transform is used [24], [25]. As the azimuthal angle φ is a periodic function, its Fourier conjugate is the OAM spectral, and the linking Fourier relationship can be described as follows

$$\begin{cases} \psi(\varphi) = \sum_{l=-\infty}^{+\infty} A_l \exp(il\varphi) \\ A_l = \dfrac{1}{2\pi} \int_{-\pi}^{\pi} d\varphi \psi(\varphi) \exp(-il\varphi), \end{cases} \tag{7}$$

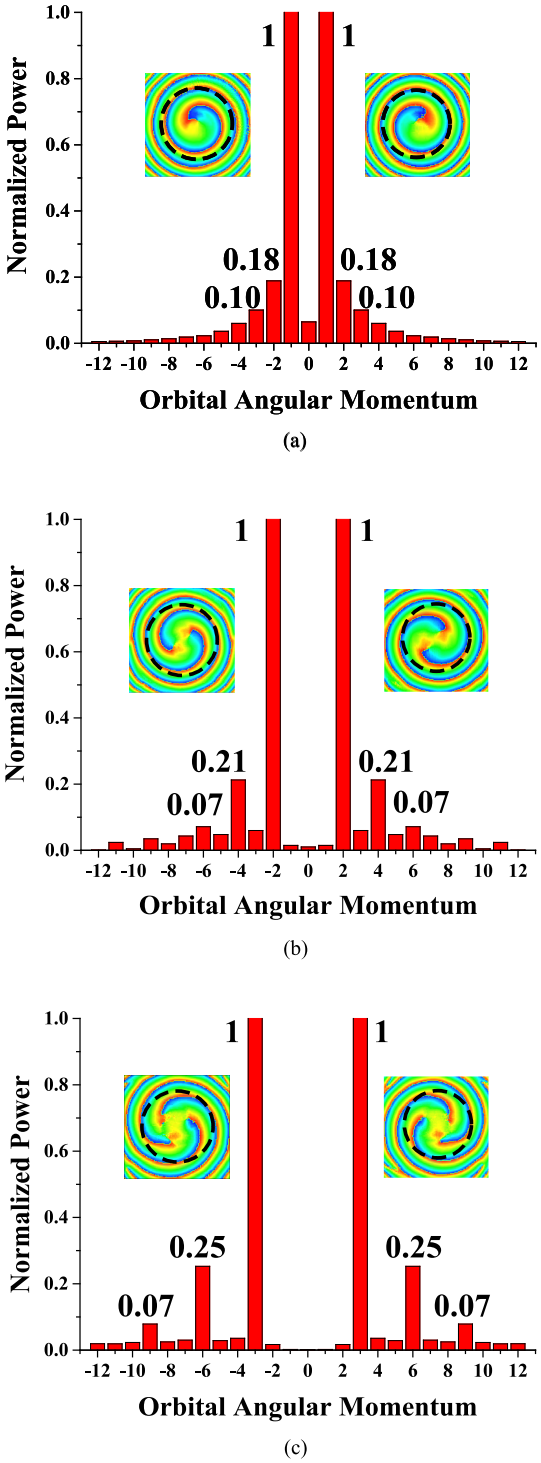

FIGURE 9. Spectrum decomposing results of different modes at $z = 13\lambda$ and $f = 2.3THz$. (a) $l = \pm 1$. (b) $l = \pm 2$. (c) $l = \pm 3$.

where ψ (φ) denotes the sampling phase and $\exp(il\varphi)$ is the spiral harmonics. Fig. 9 shows the different OAM spectra generated by the proposed reflectarray. Here the spectral intensities are normalized according to the highest spectral component. The inset is the sampling phase which is extracted along the black dotted circle perimeter. It can

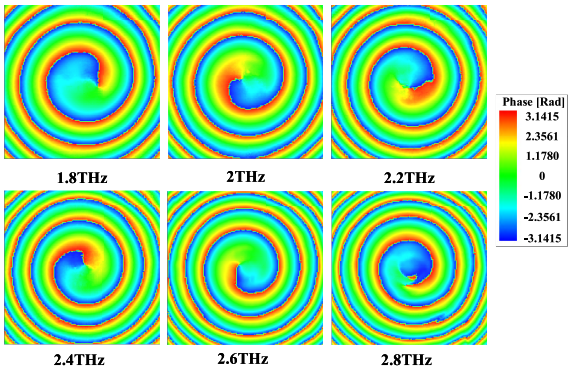

FIGURE 10. Simulated OAM beams with the $l = 1$ mode at different frequencies.

be observed that the spectral intensities of the dominant OAM modes including $l = \pm 1$, $l = \pm 2$, and $l = \pm 3$ are 82%, 79%, and 75%, respectively, which are much dominant than those of other modes, and thus good mode purity characteristic is obtained. Note that the power corresponding to the $2l$th-order OAM mode is second largest one among the spectral powers. This is because the proposed reflectarray is of 2-fold rotationally symmetry, which results in a spreading of the OAM mode [25].

In addition, as shown in Fig. 5, the reflection phase range of 360° can be achieved in a wide frequency band from 1.8THz to 2.8 THz, when the chemical potentials of the graphene sheets are suitably adjusted. Hence, the OAM vortex waves can be generated by the proposed reflectarray in a wide frequency band, as shown in Fig. 10. We can observe that the desirable spiral phase distributions can be obtained in the whole frequency band.

III. CONCLUSION

In this paper, a novel wideband tunable reflectarray is designed to generate the OAM vortex waves. The proposed metamaterial unit cell consisting of the multilayer graphene structure achieves the reflection phase range of 360° by varying the chemical potentials of the multiple graphene sheets. With the designed unit cell, the reflectarray easily generates the OAM beams with different modes including $l = \pm 1$, $l = \pm 2$, and $l = \pm 3$. With the suitable adjustment of the chemical potentials, the OAM beam can be generated in a wide frequency band from 1.8THz to 2.8THz. The proposed reflectarray provides a feasible way to efficiently generate the wideband tunable OAM beams for the wireless communication.

REFERENCES

[1] L. Allen, M. W. Beijersbergen, R. J. C. Spreeuw, and J. P. Woerdman, "Orbital angular momentum of light and the transformation of Laguerre-Gaussian laser modes," *Phys. Rev. A, Gen. Phys.*, vol. 45, no. 11, pp. 8185–8189, 1992.

[2] B. Thidé *et al.*, "Utilization of photon orbital angular momentum in the low-frequency radio domain," *Phys. Rev. Lett.*, vol. 99, no. 8, p. 087701, 2007.

[3] M. Uchida and A. Tonomura, "Generation of electron beams carrying orbital angular momentum," *Nature*, vol. 464, no. 7289, pp. 737–739, 2010.

[4] R. Niemiec, C. Brousseau, K. Mahdjoubi, O. Emile, and A. Menard, "Characterization of an OAM flat-plate antenna in the millimeter frequency band," *IEEE Antennas Propag. Lett.*, vol. 13, pp. 1011–1014, 2014.

[5] F. Capasso, P. Genevet, J. Lin, and M. A. Kats, "Holographic detection of the orbital angular momentum of light with plasmonic photodiodes," *Nature Commun.*, vol. 3, p. 1278, Dec. 2012.

[6] X. L. Cai *et al.*, "Integrated compact optical vortex beam emitters," *Science*, vol. 338, no. 6105, pp. 363–366, 2012.

[7] N. Yu *et al.*, "Light propagation with phase discontinuities: Generalized laws of reflection and refraction," *Science*, vol. 334, no. 6054, pp. 333–337, Oct. 2011.

[8] E. Karimi, S. A. Schulz, I. D. Leon, H. Qassim, J. Upham, and R. W. Boyd, "Generating optical orbital angular momentum at visible wavelengths using a plasmonic metasurface," *Light Sci. Appl.*, vol. 3, no. 5, p. e167, 2014.

[9] S. Yu, L. Li, G. Shi, C. Zhu, X. Zhou, and Y. Shi, "Design, fabrication, and measurement of reflective metasurface for orbital angular momentum vortex wave in radio frequency domain," *Appl. Phys. Lett.*, vol. 108, no. 12, p. 121904, 2016.

[10] B. Xu, C. Wu, Z. Wei, Y. C. Fan, and H. Q. Li, "Generating an orbital-angular-momentum beam with a metasurface of gradient reflective phase," *Opt. Mater. Exp.*, vol. 6, no. 12, pp. 3940–3945, 2016.

[11] L. Cheng, W. Hong, and Z. C. Hao, "Generation of electromagnetic waves with arbitrary orbital angular momentum modes," *Sci. Rep.*, vol. 4, p. 4814, Apr. 2014.

[12] Y. Chen *et al.*, "A flat-lensed spiral phase plate based on phase-shifting surface for generation of millimeter-wave OAM beam," *IEEE Antennas Wireless Propag. Lett.*, vol. 1, pp. 1156–1158, 2015.

[13] S. Yu, L. Li, G. Shi, C. Zhu, and Y. Shi, "Generating multiple orbital angular momentum vortex beams using a metasurface in radio frequency domain," *Appl. Phys. Lett.*, vol. 108, no. 24, p. 241901, 2016.

[14] E. Carrasco and J. Perruisseau-Carrier, "Reflectarray antenna at terahertz using graphene," *IEEE Antennas Wireless Propag. Lett.*, vol. 12, pp. 253–256, 2013.

[15] Y. Zhang, Y. Shi, and C.-H. Liang, "Broadband tunable graphene-based metamaterial absorber," *Opt. Mater. Exp.*, vol. 6, no. 9, pp. 3036–3043, 2016.

[16] W. Zhu, F. Xiao, M. Kang, D. Sikdar, and M. Premaratne, "Tunable terahertz left-handed metamaterial based on multi-layer graphene-dielectric composite," *Appl. Phys. Lett.*, vol. 104, no. 5, p. 051902, 2014.

[17] V. P. Gusynin, S. G. Sharapov, and J. P. Carbotte, "Magneto-optical conductivity in graphene," *J. Phys., Condens. Matter*, vol. 19, no. 2, p. 125429, 2007.

[18] V. P. Gusynin, S. G. Sharapov, and J. P. Carbotte, "Sum rules for the optical and Hall conductivity in graphene," *Phys. Rev. B, Condens. Matter*, vol. 75, no. 16, p. 165407, 2007.

[19] G. W. Hanson, "Dyadic greens functions and guided surface waves for a surface conductivity model of graphene," *J. Appl. Phys.*, vol. 103, no. 6, p. 064302, 2008.

[20] A. Vakil and N. Engheta, "Transformation optics using graphene," *Science*, vol. 332, no. 6035, pp. 1291–1294, 2011.

[21] M. Liu *et al.*, "A graphene-based broadband optical modulator," *Nature*, vol. 474, no. 7349, pp. 64–67, May 2011.

[22] J. Jin, *The Finite Element Method in Electromagnetics*. New York, NY, USA: Wiely, 2014.

[23] D. M. Pozar, *Microwave Engineering*. New York, NY, USA: Wiely, 2012.

[24] M. J. Strain *et al.*, "Fast electrical switching of orbital angular momentum modes using ultra-compact integrated vortex emitters," *Nature Commun.*, vol. 5, p. 4856, Sep. 2014.

[25] B. Jack, M. J. Padgett, and S. F. Arnold, "Angular diffraction," *New J. Phys.*, vol. 10, no. 10, p. 103013, 2008.

YAN SHI (M'07–SM'16) received the B.Eng. and Ph.D. degrees in electromagnetic fields and microwave technology from Xidian University, Xi'an, China, in 2001 and 2005, respectively.

He joined the School of Electronic Engineering, Xidian University, in 2005, and he was promoted to Full Professor in 2011. From 2007 to 2008, he was with the City University of Hong Kong, Hong Kong, China, as a Senior Research Associate. From 2009 to 2010, he was a Visiting Post-Doctoral Research Associate with the University of Illinois at Urbana-Champaign. From 2017 to 2017, he was a Visiting Professor with the State Key Laboratory of Millimeter Wave, City University of Hong Kong. He has authored or co-authored over 100 papers in referred journal and a book *Notes on Catastrophe Theory*, Beijing: Science Press, in 2015. His research interests cover computational electromagnetics, metamaterial, antenna, and electromagnetic compatibility.

Dr. Shi is a Senior Member of the Chinese Institute of Electronics. He received the Program for New Century Excellent Talents in university by the Ministry of Education of China in 2011, the New Scientific and Technological Star of Shaanxi Province by Education Department of Shaanxi Provincial Government in 2013, the First Prize of Awards for Scientific Research Results of High Education of Shaanxi Province by the Education Department of Shaanxi Provincial Government in 2013, and the Second Prize of Awards of Science and Technology by Shaanxi Province Government in 2015.

YING ZHANG received the B.E. degree in electronic engineering from Xiàn University of Posts and Telecommunications, Xi'an, China, in 2015. He is currently pursuing the master's degree in electromagnetics and microwave technology with Xidian University, Xi'an. His research interests include metamaterial and antenna designs.